DALTON

Lanthanide complexes of the tetradentate N-donor ligand dihydrobis[3-(2-pyridyl)pyrazolyl]borate and the terdentate N-donor ligand 2,6-bis(1*H*-pyrazol-3-yl)pyridine: syntheses, crystal structures and solution structures based on luminescence lifetime studies

David A. Bardwell, John C. Jeffery, Peter L. Jones, Jon A. McCleverty,* Elefteria Psillakis, Zoe Reeves and Michael D. Ward*

School of Chemistry, University of Bristol, Cantock's Close, Bristol, UK BS8 1TS

Lanthanide complexes of two polydentate N-donor ligands containing a mixture of pyridyl and pyrazolyl donors have been prepared. Dihydrobis[3-(2-pyridyl)pyrazolyl]borate $(L^1)^-$ is a tetradentate ligand with two bidentate chelating pyridyl/pyrazolyl arms linked by an apical BH_2 group; 2,6-bis(1*H*-pyrazol-3-yl)pyridine (L^2) is a terdentate chelating ligand reminiscent of terpyridine. Reaction of L^1 with lanthanide salts gave complexes of the type $[M(L^1)_2X]^{n+}$; the crystal structures of $[Eu(L^1)_2(dmf)][ClO_4]\cdot 2.5CH_2Cl_2$, $[Tb(L^1)_2(NO_3)]\cdot 2CH_2Cl_2$ and $[Tb(L^1)_2(H_2O)][L^1]\cdot H_2O\cdot 0.5CH_2Cl_2$ were determined and all contain two tetradentate ligands L^1 and an ancillary ligand X [dimethylformamide (dmf), nitrate or water] whose nature depends on the reaction/recrystallisation conditions to complete the co-ordination sphere. Luminescence studies of $[Tb(L^1)_2(NO_3)]$ in water or D_2O and MeOH or CD_3OD showed that in methanol the solvation number q is ≈1.8, consistent with displacement of nitrate by the solvent; however in water $q \approx 4.5$, indicating additional displacement of some of the N-donor heterocyclic rings of L^1 by co-ordinating water molecules. Reaction of L^2 with lanthanide salts afforded $[M(L^2)_3]^{3+}$, all isolated as their hexafluorophosphate salts. The crystal structures of three of these (M = Eu, Gd or Ho) showed that they are isostructural and isomorphous, with tricapped trigonal-prismatic nine-co-ordinate geometries similar to that of $[M(terpy)_3]^{3+}$ (terpy = 2,2′:6′,2″-terpyridine). Luminescence studies of $[Tb(L^2)_3][PF_6]_3$ gave a solvation number q of 0.6 in methanol, which is small enough to be accounted for by second-sphere solvation effects alone and therefore suggests that the nine-co-ordinate structure is retained in methanol solution. However in water, q is again ≈4.5, due to displacement of some of the donor groups of the L^2 ligands by water.

The co-ordination chemistry of lanthanides has become of increasing significance in the last few years due to the wide variety of potential applications of lanthanide complexes. Luminescent complexes of Eu^{III} and Tb^{III} may be useful in medicine as luminescent probes,[1] and highly paramagnetic complexes, generally of Gd^{III}, are used as contrast agents to enhance the output from magnetic resonance imaging (MRI) scanners.[2] In the area of supramolecular co-ordination chemistry, lanthanide ions are used as templates for the assembly of triple helicate complexes using compartmental ligands with terdentate N-donor binding sites, because of their tendency to form nine-co-ordinate complexes with three terdentate fragments.[3] The occurrence of an antenna effect, which allows sensitisation of the metal-centred luminescence *via* energy transfer from an aromatic ligand which acts as a light harvester, means that lanthanide complexes with aromatic ligands are of interest for supramolecular light-conversion devices.[4] Detailed NMR and luminescence studies have allowed determination of the relationship between solid-state and solution properties, in particular the extent of solvation.[5,6]

There is therefore considerable interest in the development of new multidentate ligands containing an aromatic chromophore for lanthanide co-ordination chemistry. To this end we recently described the co-ordination chemistry of lanthanide ions with the hexadentate N-donor podand ligand hydrotris[3-(2-pyridyl)-pyrazolyl]borate (L);[7] we found that the combination of a multidentate N-donor ligand set and a negative charge made this compound a highly effective ligand, forming complexes with both 1:1 and 1:2 (12-co-ordinate) metal:ligand ratios depending on the conditions. We describe in the first part of this paper the synthesis of the simpler tetradentate analogue dihydrobis[3-(2-pyridyl)pyrazolyl]borate (L^1), in which two bidentate chelating arms are linked at the apical anionic BH_2^- group, and the crystal structures of some of its lanthanide complexes together with some preliminary luminescence properties.

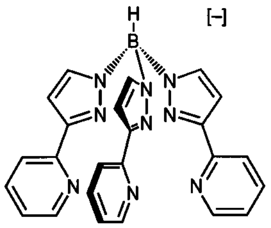
L

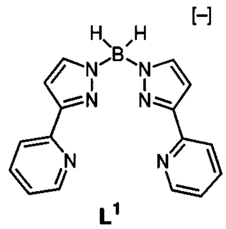
L¹

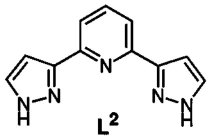
L²

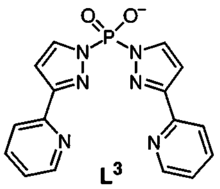
L³

In the second part of this paper we describe some homoleptic nine-co-ordinate lanthanide complexes of the terdentate N-donor ligand 2,6-bis(1*H*-pyrazol-3-yl)pyridine (L^2). As mentioned above, terdentate N-donor ligands such as 2,2′:6′,2″-terpyridine (terpy)[8] and various structural analogues[9–11] have been of particular interest in lanthanide co-ordination chemistry because of their structural and photophysical properties. The preparation of L^2 was reported a while ago,[12] but as far as we are aware the only co-ordination chemistry that has been described with it was the study of a mononuclear iron(II) complex showing spin-crossover behaviour.[13] The crystal structures of the complexes and some preliminary luminescence studies are described.

Experimental

Instrumentation used for standard spectroscopic and analytical studies has been described previously.[7] 3-(2-Pyridyl)pyrazole and 2,6-bis(pyrazol-3-yl)pyridine (L^2) were prepared according to the literature method.[12]

Luminescence spectra were recorded using a Perkin-Elmer LS-50B spectrofluorimeter equipped with a Hamamatsu R928 photomultiplier tube, using excitation and emission slit widths of 5–12 nm depending on the intensity of the emission. Phosphorescence lifetimes (τ) were measured with the instrument in time-resolved mode, and are the average of at least three independent measurements which were made by monitoring the decay at a wavelength corresponding to the maximum intensity of the emission spectrum (546 nm for Tb), following pulsed excitation. The intensity of the emission after the pulsed excitation was monitored after 20 different delay times spanning at least two lifetimes. The resulting first-order decay curves gave linear plots of ln *I vs. t* from which the lifetime was calculated by $\tau = (\ln 2)/\text{slope}$. The number of co-ordinated solvent molecules (q) for the terbium(III) complexes was calculated from the Horrocks equation, $q = n(\tau_H^{-1} - \tau_D^{-1})$, where τ_H is the lifetime in the protonated solvent, (water or MeOH), τ_D that lifetime in the corresponding deuteriated solvent, and the values of n are 4.2 (Tb in water–D_2O) or 8.4 (Tb in MeOH–CD_3OD).[6]

Preparations

Potassium dihydrobis[3-(2-pyridyl)pyrazolyl]borate KL^1. A mixture of 3-(2-pyridyl)pyrazole (3.50 g, 24.1 mmol) and KBH_4 (0.49 g, 9.0 mmol) was ground together finely with a mortar and pestle and then gradually heated to 150 °C. Melting occurred at *ca.* 120 °C, at which point evolution of H_2 commenced. The temperature was maintained at 150 °C for 30 min, after which time evolution of H_2 had ceased. The solid white mixture was cooled and warm toluene (100 cm^3) was added. The suspension was stirred vigorously overnight to allow the excess of unreacted 3-(2-pyridyl)pyrazole to dissolve. The product was filtered off as a white solid, which was washed further with several portions of toluene and then hexane and dried. Yield of KL^1: 2.48 g (81%). Negative-ion FAB mass spectrum: *m/z* 301 [$(L^1)^-$]. NMR [$(CD_3)_2CO$] ^1H, δ 8.51 (1 H, ddd, *J* 4.9, 1.7, 1.0, pyridyl H^6), 7.8–7.7 (2 H, m, pyridyl H^3, H^4), 7.54 (1 H, d, *J* 2.0, pyrazolyl H^5), 7.13 (1 H, ddd, *J* 7.3, 4.9, 1.5, pyridyl H^5) and 6.59 (1 H, d, *J* 2.0 Hz, pyrazolyl H^4); ^{13}C, δ 155.1, 151.7, 150.1, 137.3, 136.3, 122.0, 120.8 and 102.6. ν_{BH}(KBr disc): 2378, 2349, 2318 and 2254 cm^{-1} (Found: C, 55.8; H, 4.2; N, 24.7. Calc. for $C_{16}H_{14}BN_6K$: C, 56.5; H, 4.1; N, 24.7%).

$[Eu(L^1)_2(dmf)][ClO_4]$. To a solution of $EuCl_3{\cdot}6H_2O$ (0.055 g, 0.15 mmol) in methanol (20 cm^3) was added a solution of KL^1 (0.1 g, 0.29 mmol) in methanol (20 cm^3). After stirring for 1 h, aqueous $NaClO_4$ (excess) was added to give a white precipitate which was filtered off and dried. Recrystallisation from dimethylformamide (dmf)–diethyl ether afforded 0.064 g (46%) of the product as a white powder. X-Ray-quality crystals of $[Eu(L^1)_2(dmf)][ClO_4]{\cdot}2.5CH_2Cl_2$ were grown from CH_2Cl_2–hexane mixtures.

$[Tb(L^1)_2(NO_3)]$. To a solution of $Tb(NO_3)_3{\cdot}5H_2O$ (0.128 g, 0.30 mmol) in methanol (20 cm^3) was added a solution of KL^1 (0.20 g, 0.59 mmol) in methanol (20 cm^3). The mixture was allowed to stir for 1 h, and then water was added until precipitation of the product as a white solid was complete. The fine white precipitate was extracted with several portions of CH_2Cl_2 which were combined, dried, and evaporated to dryness to give $[Tb(L^1)_2(NO_3)]$ in 0.20 g (81%) yield. X-Ray-quality crystals of $[Tb(L^1)_2(NO_3)]{\cdot}2CH_2Cl_2$ were grown from CH_2Cl_2–hexane.

$[Tb(L^1)_2(H_2O)][L^1]{\cdot}H_2O$. To a solution of $TbCl_3{\cdot}6H_2O$ (0.055 g, 0.15 mmol) in methanol (20 cm^3) was added a solution of KL^1 (0.1 g, 0.29 mmol) in methanol (20 cm^3). After stirring for 1 h, the product was precipitated by addition of water. The fine white precipitate was extracted with several portions of CH_2Cl_2 which were combined, dried, and evaporated to dryness. Recrystallisation from CH_2Cl_2–hexane afforded $[Tb(L^1)_2(H_2O)][L^1]{\cdot}H_2O{\cdot}0.5CH_2Cl_2$ as colourless X-ray-quality crystals (0.063 g, 39%).

$[M(L^2)_3][PF_6]_3$ (M = Eu, Gd, Tb or Ho). A solution of the appropriate $MCl_3{\cdot}6H_2O$ (0.33 mmol) and L^2 (0.21 g, 1 mmol) in methanol (10 cm^3) was stirred for 30 min. A solution of an excess of KPF_6 in water was then added, resulting in a white precipitate. After overnight cooling to allow complete precipitation, the solid was filtered off and dried *in vacuo* to afford $[M(L^2)_3][PF_6]_3$ in 75–90% yield. The crude materials were readily crystallised by slow evaporation from methanol to give X-ray-quality crystals.

Mass spectra and elemental analyses for all of the complexes are summarised in Table 1.

Crystallography

Suitable crystals were quickly transferred from the mother-liquor to a stream of cold N_2 at -100 °C on a Siemens SMART diffractometer fitted with a CCD-type area detector. A detailed experimental description of the methods used for data collection and integration using the SMART system has been published.[7] Table 2 contains a summary of the crystal parameters, data collection and refinement. In all cases the structures were solved by conventional heavy-atom or direct methods and refined by the full-matrix least-squares method on all F^2 data using the SHELXTL 5.03 package on Silicon Graphics Indigo-R4000 or Indy computers.[14] Non-hydrogen atoms were refined with anisotropic thermal parameters; hydrogen atoms were included in calculated positions and refined with isotropic thermal parameters.

Crystals of $[Eu(L^1)_2(dmf)][ClO_4]{\cdot}2.5CH_2Cl_2$ were needles for which an accurate absorption correction was difficult, resulting in significant residual peaks in the final electron-density map close to the metal centre. Apart from one complex formula unit, the asymmetric unit contains 2.5 molecules of CH_2Cl_2 of which the half molecule is disordered across an inversion centre. The disorder is such that the two Cl atoms are ordered, but the carbon atom [C(30)] occurs in two positions with equal site occupation factors. Hydrogen atoms were not included for the disordered carbon atom.

The structure of $[Tb(L^1)_2(H_2O)][L^1]{\cdot}H_2O{\cdot}0.5CH_2Cl_2$ showed a remarkable amount of disorder in the positions of many of the atoms of the L^1 ligands (see Figs. 2 and 3). This arises from two significantly different conformers which are present in the crystal. The disordered atoms could be separated into two sets; refinement of the fractional site occupancies of the two sets converged at approximately 50 : 50 so the site occupancies were fixed at that value in the final refinement. The co-ordinated N atoms of the ligands L^1 were common to both conformers; the two conformations are generated by movement of the aromatic rings about their point of attachment to the metal.

The structural determination of $[Tb(L^1)_2(NO_3)]{\cdot}2CH_2Cl_2$ presented no problems.

The three compounds $[M(L^2)_3][PF_6]_3$ (M = Eu, Gd or Ho) are isostructural and isomorphous, all crystallising in space group *C*2/*c* such that the complex cation and one of the hexafluorophosphate anions lie astride C_2 axes. The hexafluorophosphate anions were disordered in the same manner in every case, but the two disordered components could be successfully resolved. In $[Gd(L^2)_3][PF_6]_3$ isotropic restraints were applied to fluorine atoms F(11′), F(12′) and F(14′) (where the prime denotes the minor component of the disorder) to keep the refinement stable.

Atomic coordinates, thermal parameters, and bond lengths

Table 1 Analytical and mass spectroscopic data for the new complexes

Complex	Elemental analyses (%)[a]			FAB mass spectral data [*m/z*, relative intensity (%), assignment]		
$[Eu(L^1)_2(dmf)][ClO_4]$	45.0 (45.4)	3.4 (3.7)	19.6 (19.7)	906	3	*b*
				755	100	$[Eu(L^1)_2]^+$
				597	30	$[EuL^1(pypz)]^+$ [c]
				454	25	$[EuL^1]^+$
				297	32	$[Eu(pypz)]^+$
$[Tb(L^1)_2(NO_3)]$	46.0 (46.6)	3.4 (3.4)	21.6 (22.1)	761	100	$[Tb(L^1)_2]^+$
				604	30	$[TbL^1(pypz)]^+$
				447	24	$[Tb(pypz)_2]^+$
$[Tb(L^1)_2(H_2O)][L^1]\cdot H_2O$	48.8 (48.5)	3.7 (4.0)	20.5 (20.6)[d]	912	3	*b*
				761	100	$[Tb(L^1)_2]^+$
$[Eu(L^2)_3][PF_6]_3$	33.4 (32.5)	2.4 (2.2)	18.0 (17.2)	784	28	$[EuL^2(L^2 - H)_2]^+$
				613	52	$[Eu(L^2)_2F_2]^+$
				593	38	$[EuL^2(L^2 - H)F]^+$
				573	100	$[Eu(L^2 - H)_2]^+$
$[Gd(L^2)_3][PF_6]_3$	31.3 (32.3)	2.3 (2.2)	16.7 (17.1)	1081	4	$[Gd(L^2)_3(PF_6)_2]^+$
				935	10	$[Gd(L^2)_2(L^2 - H)(PF_6)]^+$
				789	64	$[GdL^2(L^2 - H)_2]^+$
				618	50	$[Gd(L^2)_2F_2]^+$
				598	38	$[GdL^2(L^2 - H)F]^+$
				578	100	$[Gd(L^2 - H)_2]^+$
$[Tb(L^2)_3][PF_6]_3$	31.7 (32.3)	2.1 (2.2)	16.7 (17.1)	1083	4	$[Tb(L^2)_3(PF_6)_2]^+$
				790	56	$[TbL^2(L^2 - H)_2]^+$
				619	45	$[Tb(L^2)_2F_2]^+$
				599	35	$[TbL^2(L^2 - H)F]^+$
				579	100	$[Tb(L^2 - H)_2]^+$
$[Ho(L^2)_3][PF_6]_3$	32.8 (32.1)	2.2 (2.2)	17.7 (17.0)	796	22	$[HoL^2(L^2 - H)_2]^+$
				625	60	$[Ho(L^2)_2F_2]^+$
				605	34	$[HoL^2(L^2 - H)F]^+$
				585	100	$[Ho(L^2 - H)_2]^+$

[a] Calculated values in parentheses. [b] This peak is at 151 mass units above the parent ion $[M(L^1)_2]^+$. The matrix (3-nitrobenzyl alcohol) has a relative molecular mass of 153; the peaks are therefore most likely due to a matrix adduct of some sort. [c] pypz = 3-(2-Pyridyl)pyrazole, the bidentate 'arm' arising from fragmentation of the ligand L^1 (see text). [d] Analysis calculated with 1.5 molecules of CH_2Cl_2; the sample for analysis was crystallised from this solvent.

and angles have been deposited at the Cambridge Crystallographic Data Centre (CCDC). See Instructions for Authors, *J. Chem. Soc.*, *Dalton Trans.*, 1997, Issue 1. Any request to the CCDC for this material should quote the full literature citation and the reference number 186/500.

Results and Discussion

Synthesis of L^1

The new ligand L^1 was prepared by reaction of 3-(2-pyridyl)pyrazole with KBH_4, in a 2.5:1 ratio and at a temperature (150 °C) such that formation of the bis(pyrazolyl)borate occurred readily but further reaction to give the tris(pyrazolyl)borate did not. This synthesis follows the usual route for preparing bidentate bis(pyrazol-1-yl)borates from substituted pyrazoles.[15,16] Compound L^1 therefore has two bidentate arms linked by a flexible BH_2^- spacer, and we can envisage two different co-ordination modes for this ligand. Depending on the charge and stereoelectronic preferences of the metal ion, it could (*i*) co-ordinate as a tetradentate ligand to a single metal ion, or (*ii*) act as a bis-bidentate bridge, co-ordinating each arm to a different metal ion, which generally leads to formation of polynuclear helicates.[16,17] For example with the related ligand bis[3-(2-pyridyl)pyrazol-1-yl]phosphinate (L^3), which is similar to L^1 but contains a phosphinate PO_2^- bridge instead of BH_2^-, both types of co-ordination have been observed.[17]

Syntheses and structures of lanthanide complexes of L^1

Reaction of L^1 (as its potassium salt) with lanthanide(III) salts (nitrate, chloride) resulted in complexes of the form $[LnL^1_2X]^{n+}$. In all cases two ligands L^1 are co-ordinated to a single metal centre, which accounts for eight co-ordination sites. The remaining site(s) and the nature of the anion varied with the details of the synthesis and recrystallisation.

Reaction of $EuCl_3\cdot 6H_2O$ with 2 equivalents of KL^1 in methanol, followed by precipitation as the perchlorate salt and recrystallisation from dmf–ether, afforded $[Eu(L^1)_2(dmf)][ClO_4]$. Initially the ninth co-ordination site is probably occupied by water, which is replaced by dmf during crystallisation. Further subsequent recrystallisation from the non-co-ordinating solvent mixture CH_2Cl_2–hexane did not result in displacement of the dmf ligand. In contrast, reaction of $Tb(NO_3)_3\cdot 5H_2O$ with 2 equivalents of KL^1 under the same conditions resulted in formation of neutral $[Tb(L^1)_2(NO_3)]$ in which the nitrate counter ion is retained in the co-ordination sphere of the Tb^{III}. We were then interested to see what would happen in the absence of both nitrate and any other added anions. Reaction of $TbCl_3\cdot 6H_2O$ with 2 equivalents of KL^1 in methanol followed by the addition of water to precipitate a white solid yielded $[Tb(L^1)_2(H_2O)][L^1]\cdot H_2O$, in which a 'free' molecule of L^1 (associated with a water molecule) is acting as the counter ion.

All of these complexes were characterised by FAB mass spectroscopy, elemental analyses, and finally X-ray crystallography. In all of the FAB mass spectra (Table 1) the most intense peak corresponded to $[Ln(L^1)_2]^+$, in which the ancillary ligands (nitrate, water, dmf) have dissociated. Lower-mass peaks were generally observed due to fragmentation of L^1 by cleavage of the B–N bonds, leaving bidentate 3-(2-pyridyl)pyrazole fragments attached to the metal centre.

The crystal structure of $[Eu(L^1)_2(dmf)][ClO_4]\cdot 2.5CH_2Cl_2$ is shown in Fig. 1; selected bond lengths and angles are in Table 3. The two ligands L^1 are acting as tetradentate chelates, in the manner of the hexadentate podand L but with one bidentate arm missing. The ninth co-ordination site is occupied by an O-donor dmf molecule. As with the lanthanide complexes of L,[7]

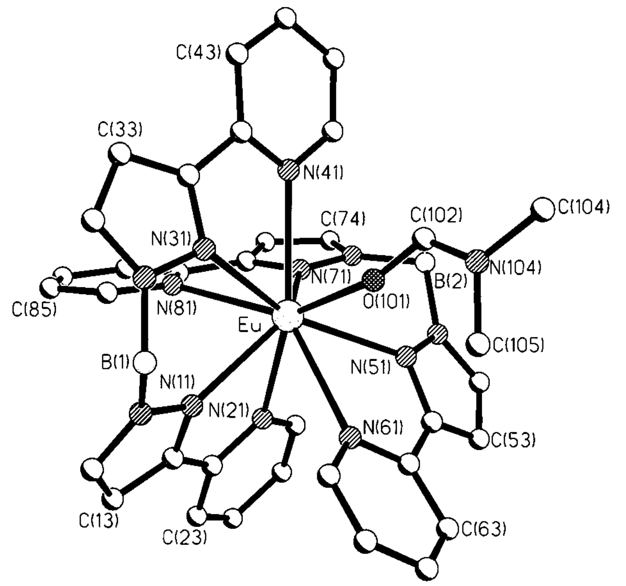

Fig. 1 Crystal structure of the complex cation of $[Eu(L^1)_2(dmf)][ClO_4]\cdot 2.5CH_2Cl_2$

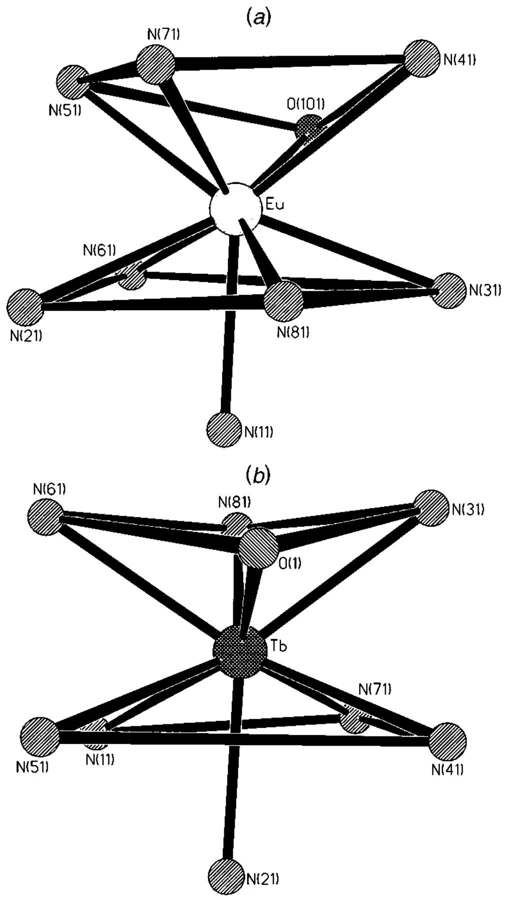

Fig. 2 Co-ordination geometries of the metal centres in (*a*) $[Eu(L^1)_2(dmf)][ClO_4]\cdot 2.5CH_2Cl_2$ and (*b*) $[Tb(L^1)_2(H_2O)][L^1]\cdot H_2O\cdot 0.5CH_2Cl_2$

the bonds from Eu to the pyrazolyl N donors (2.52–2.60 Å) are rather shorter than those to the pyridyl N donors (2.63–2.72 Å). Each ligand L^1 is not planar, but folded due to the tetrahedral geometry of the apical boron atoms, which have N–B–N angles very close to the tetrahedral ideal. The geometry about the metal ion approximates to that of a capped square antiprism [Fig. 2(*a*)], with N(51), N(71), N(41) and O(101) forming the top plane, N(21), N(61), N(31) and N(81) forming the bottom plane and N(11) capping the bottom plane. For the N(51), N(71), N(41), O(101) set the displacements from the mean plane through them are −0.168, +0.173, −0.170 and +0.165 Å respectively. The N(21), N(61), N(31), N(81) set forms a more accurate plane, with the displacements of the atoms from the mean plane through them being +0.076, −0.055, +0.055 and −0.076 Å respectively. The angle of intersection between the two mean planes is 9°.

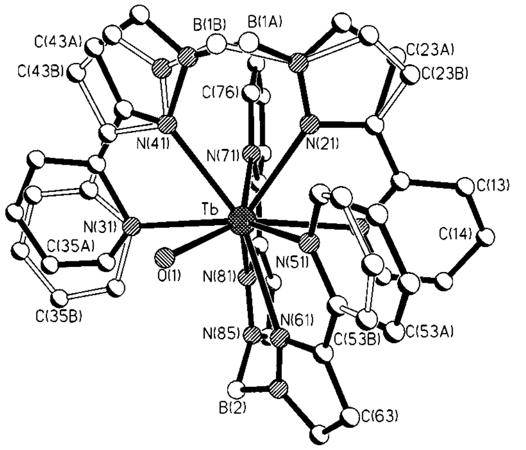

Fig. 3 Crystal structure of the complex cation of $[Tb(L^1)_2(H_2O)][L^1]\cdot H_2O\cdot 0.5CH_2Cl_2$, showing the two disordered components

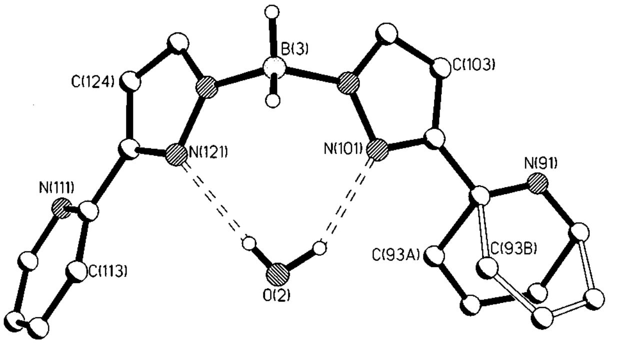

Fig. 4 Crystal structure of the complex anion of $[Tb(L^1)_2(H_2O)][L^1]\cdot H_2O\cdot 0.5CH_2Cl_2$, showing the two disordered components

The structure (Figs. 3 and 4, Table 4) of the $[Tb(L^1)_2(H_2O)]^+$ cation of $[Tb(L^1)_2(H_2O)][L^1]\cdot H_2O\cdot 0.5CH_2Cl_2$ is similar to that of $[Eu(L^1)_2(dmf)]^+$ (above). Again it contains two tetradentate L^1 ligands and one monodentate O-donor (water) making a similar nine-co-ordinate geometry, which again may be described as a capped square antiprism [Fig. 2(*b*)]. In this case the 'top' plane is described by the donor atoms O(1), N(61), N(81), N(31), which have displacements of +0.137, −0.133, +0.139 and −0.143 Å respectively from the mean plane through them. The 'bottom' plane is described by N(11), N(71), N(41), N(51), which have displacements of +0.077, −0.077, +0.058 and −0.058 Å respectively from the mean plane through them. Atom N(21) caps the bottom plane; the angle of intersection between the two mean planes is 7°. In this structure the anion is of particular interest, being a free L^1 which encloses a water molecule hydrogen bonded to the two pyrazolyl nitrogen atoms (Fig. 4). The non-bonded distances O(2)···N(101) and O(2)···N(121) are 2.943 and 2.899 Å respectively which are typical distances for O–H···N hydrogen bonds.[18,19] This is a nice example of a host–guest type interaction *via* multipoint hydrogen bonding, with an ideal complementarity between the geometric arrangement of the hydrogen-bond donors of the guest (the water O–H bonds) and the hydrogen-bond acceptors of the host (the pyrazolyl N atoms). One of the pyridyl rings of the complex anion $[L^1\cdot H_2O]^-$ is involved in a hydrogen-bonding interaction with the co-ordinated water on the complex cation, *i.e.* Tb–OH_2···N (pyridyl), with a non-bonded O(1)···N(111) separation of 2.770 Å.

A particular problem with this structure was the presence of a 50:50 disorder between two different conformations of

Table 2 Summary of crystal parameters, data collection and refinement for the six crystal structures[a]

	$[Eu(L^1)_2(dmf)]$-$[ClO_4]\cdot2.5CH_2Cl_2$	$[Tb(L^1)_2(NO_3)]\cdot$$2CH_2Cl_2$	$[Tb(L^1)_2(H_2O)][L^1]\cdot$$H_2O\cdot0.5CH_2Cl_2$	$[Eu(L^2)_3][PF_6]_3$	$[Gd(L^2)_3][PF_6]_3$	$[Ho(L^2)_3][PF_6]_3$
Formula	$C_{37.5}H_{40}B_2Cl_6$-$EuN_{13}O_4$	$C_{34}H_{32}B_2Cl_4N_{13}O_3$-Tb	$C_{48.5}H_{46}B_3ClN_{18}$-$O_2Tb$	$C_{33}H_{27}EuF_{18}N_{15}P_6$	$C_{33}H_{27}F_{18}GdN_{15}P_6$	$C_{33}H_{27}F_{18}HoN_{15}P_6$
M	1139.10	993.07	1139.83	1220.57	1225.86	1233.54
Space group	$P2_1/n$	$P2_1/n$	$P2_1/c$	$C2/c$	$C2/c$	$C2/c$
a/Å	12.207(2)	10.3520(7)	12.167(2)	16.150(2)	16.134(2)	16.142(3)
b/Å	12.124(2)	21.792(2)	18.901(2)	21.274(2)	21.251(3)	21.210(2)
c/Å	31.498(6)	17.818(2)	22.224(2)	12.710(3)	12.697(2)	12.685(2)
β/°	98.02(2)	99.971(7)	91.207(10)	95.396(14)	95.42(2)	95.470(12)
U/Å^3	4616.0(14)	3959.0(6)	5109.8(8)	4347.5(5)	4334.0(10)	4323.3(1)
D_c/g cm^{-3}	1.639	1.666	1.482	1.865	1.879	1.895
μ/mm^{-1}	1.764	2.110	1.495	1.679	1.77	2.068
F(000)	2284	1976	2304	2400	2404	2416
Crystal size/mm	0.4 × 0.3 × 0.1	0.45 × 0.3 × 0.3	0.4 × 0.2 × 0.15	0.25 × 0.2 × 0.1	0.3 × 0.2 × 0.1	0.2 × 0.15 × 0.1
Reflections collected: total, independent, R_{int}	27 933, 10 398, 0.061	25 068, 9000, 0.025	51 516, 11 696, 0.038	12 384, 4726, 0.051	13 794, 4964, 0.108	13 630, 4940, 0.038
Data, restraints, parameters	10 396, 0, 586	8999, 0, 514	11 695, 27, 847	4726, 0, 374	4962, 48, 359	4940, 0, 374
Final $R1$, $wR2$[b,c]	0.066, 0.202	0.023, 0.059	0.063, 0.134	0.038, 0.071	0.058, 0.129	0.028, 0.055
Weighting factors[c]	0.1180, 0	0.0319, 0	0, 25.5765	0.0293, 0	0.0541, 0	0.0218, 0
Largest peak, hole/e Å^{-3}	2.492, −3.671	+0.874, −0.746	+1.209, −1.591	+0.669, −1.107	+1.436, −1.853	+0.480, −0.594

[a] Details in common: graphite-monochromatised Mo-Kα radiation, $\bar{\lambda} = 0.710\,73$ Å; 2θ limits for data collection, 3–55°; temperature for data collection, 173 K; monoclinic; $Z = 4$. [b] Structure was refined on F_o^2 using all data; the value of $R1$ is given for comparison with older refinements based on F_o with a typical threshold of $F \geqslant 4\sigma(F)$. [c] $wR2 = [\Sigma w(F_o^2 - F_c^2)^2/\Sigma w(F_o^2)^2]^{\frac{1}{2}}$ where $w^{-1} = [\sigma^2(F_o^2) + (aP)^2 + bP]$ and $P = [\max(F_o^2, 0) + 2F_c^2]/3$.

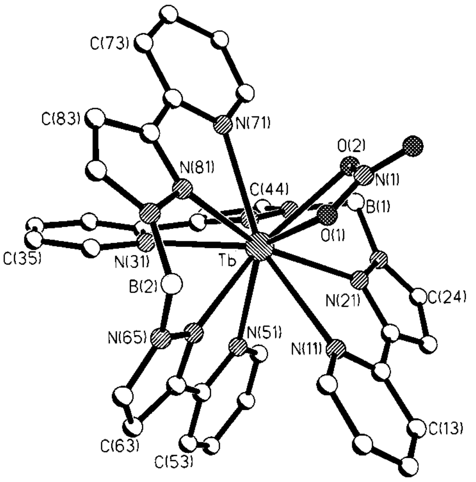

Fig. 5 Crystal structure of the complex unit of $[Tb(L^1)_2(NO_3)]\cdot2CH_2Cl_2$

Table 3 Selected bond lengths (Å) and angles (°) for $[Eu(L^1)_2(dmf)]$-$[ClO_4]\cdot2.5CH_2Cl_2$

Eu–O(101)	2.360(5)	Eu–N(81)	2.627(6)
Eu–N(11)	2.516(6)	Eu–N(21)	2.651(6)
Eu–N(71)	2.531(5)	Eu–N(61)	2.692(5)
Eu–N(51)	2.587(6)	Eu–N(41)	2.718(6)
Eu–N(31)	2.596(6)		
N(11)–Eu–N(21)	64.3(2)	N(11)–Eu–N(31)	72.1(2)
N(31)–Eu–N(41)	61.9(2)	N(21)–Eu–N(41)	140.6(2)
N(51)–Eu–N(61)	62.4(2)	N(71)–Eu–N(51)	71.3(2)
N(71)–Eu–N(81)	64.1(2)	N(81)–Eu–N(61)	137.1(2)
O(101)–Eu–N(61)	70.2(2)	O(101)–Eu–N(41)	73.0(2)

Table 4 Selected bond lengths (Å) and angles (°) for $[Tb(L^1)_2(H_2O)]$-$[L^1]\cdot H_2O\cdot0.5CH_2Cl_2$

Tb–O(1)	2.353(5)	Tb–N(11)	2.599(6)
Tb–N(21)	2.520(7)	Tb–N(71)	2.622(6)
Tb–N(81)	2.524(6)	Tb–N(31)	2.648(8)
Tb–N(41)	2.564(8)	Tb–N(51)	2.686(7)
Tb–N(61)	2.595(6)		
N(41)–Tb–N(31)	62.8(3)	N(21)–Tb–N(41)	71.6(3)
N(21)–Tb–N(11)	64.6(2)	N(11)–Tb–N(31)	140.5(2)
N(61)–Tb–N(51)	62.4(2)	N(81)–Tb–N(61)	71.8(2)
N(81)–Tb–N(71)	64.7(2)	N(71)–Tb–N(51)	138.9(2)
O(1)–Tb–N(31)	71.2(2)	O(1)–Tb–N(51)	71.6(2)

several of the heterocyclic rings in both the complex cation and the complex anion. This is illustrated in Figs. 3 and 4. In one of the co-ordinated L^1 ligands of the cation one pyridyl ring has two slightly different orientations with the site of attachment to the metal ion [N(51)] being common to both. The second co-ordinated L^1 is more disordered with both of the pyrazolyl rings, the apical boron atom and one of the pyridyl rings exhibiting disorder over two positions (Fig. 3). It should be emphasised that since the sites of attachment of the heterocyclic rings to the metal ion are common to both components the geometry about the metal ion is the same in each case. In the complex anion $[L^1\cdot H_2O]^-$ one of the pyridyl rings exhibits this two-fold disorder (Fig. 4). Despite the extensive disorder, the components could be satisfactorily resolved and the overall level of refinement is quite reasonable ($R1 = 0.063$).

The crystal structure of $[Tb(L^1)_2(NO_3)]\cdot2CH_2Cl_2$ is in Fig. 5; selected bond lengths and angles are in Table 5. The structure of the complex is similar to those above with the exception that a bidentate nitrate ion has replaced the monodentate (dmf or water) ligand. This has a noticeable effect on the complex structure, as the bidentate nitrate ligand has a greater sterically hindering effect close to the metal ion than do the monodentate ligands of the first two complexes. This is illustrated in Fig. 6, which shows alternative views of all three complexes: the two bidentate arms of the L^1 ligands which lie near the ancillary ligand are obviously repelled from the nitrate ion more than they are from the monodentate ligands. This effect may be quantified by measuring the angle between the mean planes of these two bidentate (pyridylpyrazolyl) arms. In the above two structures, with monodentate dmf and H_2O ligands, the angles between these two ligand fragments are 150 and 164° respectively; in $[Tb(L^1)_2(NO_3)]$ it is 173°. Similarly, the bonds from Tb

Table 5 Selected bond lengths (Å) and angles (°) for $[Tb(L^1)_2(NO_3)]\cdot 2CH_2Cl_2$

Tb–O(1)	2.494(2)	Tb–N(81)	2.622(2)
Tb–N(41)	2.512(2)	Tb–N(51)	2.624(2)
Tb–N(61)	2.521(2)	Tb–N(31)	2.637(2)
Tb–O(2)	2.538(2)	Tb–N(71)	2.736(2)
Tb–N(21)	2.602(2)	Tb–N(11)	2.797(2)
N(21)–Tb–N(11)	60.39(6)	N(41)–Tb–N(21)	71.45(6)
N(41)–Tb–N(31)	64.23(6)	N(31)–Tb–N(11)	132.17(6)
N(61)–Tb–N(51)	64.32(6)	N(61)–Tb–N(81)	70.56(6)
N(81)–Tb–N(71)	60.37(6)	N(51)–Tb–N(71)	132.43(6)
O(1)–Tb–N(71)	91.14(6)	O(2)–Tb–N(71)	65.92(6)
O(1)–Tb–N(11)	66.26(6)	O(2)–Tb–N(11)	93.12(6)
O(1)–Tb–O(2)	50.46(6)		

to the pyridyl N atoms N(11) and N(71) are significantly longer (0.14 Å on average) than those to N(31) and N(51), which may be ascribed to their proximity to the bidentate nitrate ligand.

Solution luminescence properties of $[TbL^1_2(NO_3)]$

The luminescence properties of lanthanide complexes in solution, particularly those of Tb^{III} and Eu^{III}, can give useful information regarding their solution structures.[5,6] To this end we examined $[Tb(L^1)_2(NO_3)]$ as a representative member of this series of complexes. The results are summarised in Table 6.

We showed earlier from conductivity studies with $[TbL(NO_3)_2]$ that the neutral molecule remained intact in CH_2Cl_2 solution, but dissociated in water to give $[TbL(H_2O)_q]^{2+}$ ($q \approx 3.6$) and two nitrate ions, and was therefore soluble in both hydrophobic and hydrophilic solvents.[7] We would therefore expect similar behaviour from $[Tb(L^1)_2(NO_3)]$, and indeed found it to be significantly soluble in both CH_2Cl_2 and water. The complex dissolves in CH_2Cl_2 solution as a neutral molecule with retention of the co-ordinated nitrate. The electronic spectrum contains ligand-centred $\pi \longrightarrow \pi^*$ transitions at $\lambda_{max} =$ 295 and 254 nm, and excitation at either of these wavelengths gives an entirely typical and extremely intense terbium(III) emission spectrum containing the expected sequence of $^5D_4 \longrightarrow {}^7F_n$ transitions, with the $n = 6$, 5, 4 and 3 components being visible.[7] The half-life τ of this emission is 1.32 ms.

Comparison of the luminescence lifetimes of $[Tb(L^1)_2(NO_3)]$ in water and D_2O allows an estimation of the value of q, the number of co-ordinated water molecules in the hydrated species, because of the differing abilities of the O–H and O–D oscillators to quench the metal-based excited state.[6] Similarly, measurements in MeOH and MeOD allow estimation of the number of co-ordinated methanol molecules. Considering the methanol solutions first, the difference between the τ values (1.18 ms in MeOH and 1.57 ms in CD_3OD) gives $q = 1.8 \pm 0.5$ (the error of ± 0.5 is generally assumed to be reasonable for this calculation).[6] This is consistent with either two co-ordinated methanol molecules (10-co-ordinate metal centre), or with one directly co-ordinated methanol (nine-co-ordinate metal centre) and additional contributions to solvent-based quenching arising from second-sphere interactions. It has been shown by Parker and co-workers[20] that, even in complexes with no solvent molecules *directly* co-ordinated to the lanthanide centre, second-sphere co-ordination and/or hydrogen bonding of solvent molecules to the ligand can still lead to significant lifetime differences between protonated and deuteriated solvents, leading to apparent q values anywhere between 0 and 1. The complex $[Tb(L^1)_2(NO_3)]$ therefore dissociates in methanol to give $[Tb(L^1)_2(MeOH)_q]^+$ where the value of 1.8 ± 0.5 for q may reasonably be ascribed to one directly co-ordinated methanol molecule with additional second-sphere solvent effects also providing significant quenching.

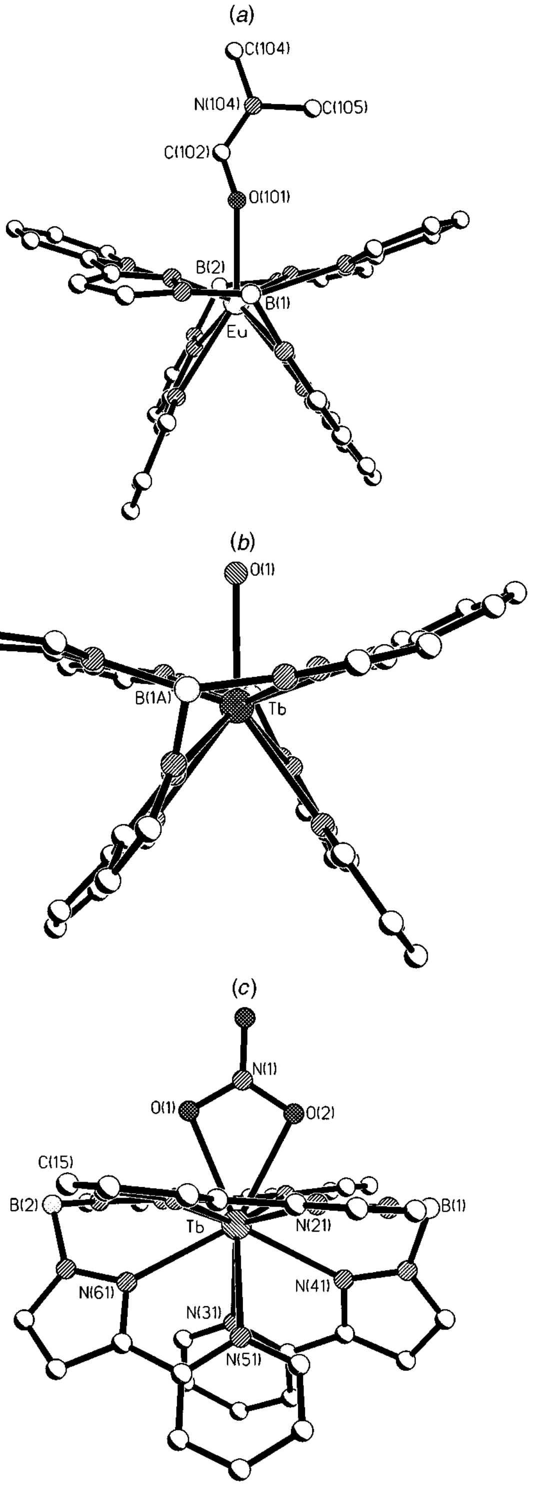

Fig. 6 Alternative views of the three structures, emphasising the effect of the steric bulk of the ancillary ligands on the geometries of the complexes

The results in water and D_2O were significantly different. The difference between the τ values (0.58 ms in water and 1.56 ms in D_2O) gives $q = 4.5 \pm 0.5$. Such a large extent of hydration cannot be accounted for just by dissociation of one nitrate ion, which would permit co-ordination of one or two water molecules (*cf.* the results in methanol, above). It therefore appears that dissolution of $[Tb(L^1)_2(NO_3)]$ in water results in dissociation of one or more of the heterocyclic rings in addition to nitrate dissociation. Such behaviour has been established in $[Eu(terpy)_3]^{3+}$, which in MeCN solution can undergo a ligand-based conformational rearrangement involving rotation of terminal pyridyl rings about the interannular C–C bonds.[21] The *cis,cis* conformation (terdentate terpyridine) can become *cis, trans* (bidentate terpyridine) or even *trans,trans* (monodentate

Table 6 Luminescence lifetimes (ms) of terbium(III) complexes in different solvents[a]

Complex	CH_2Cl_2	MeOH	CD_3OD	Water	D_2O
$[Tb(L^1)_2(NO_3)]$	1.32	1.18	1.57	0.58	1.56
$[Tb(L^2)_3][PF_6]_3$	1.46	1.09	1.18	0.45[b]	0.88[b]

[a] Estimated error on lifetimes ±0.02 ms, except where stated otherwise.
[b] Decay not single exponential: estimated error in lifetimes ±0.1 ms.

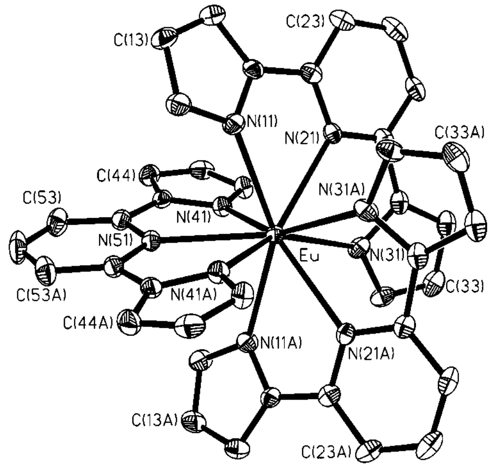

Fig. 7 Crystal structure of the complex cation of $[Eu(L^2)_3][PF_6]_3$; the complexes of Gd and Ho are isostructural

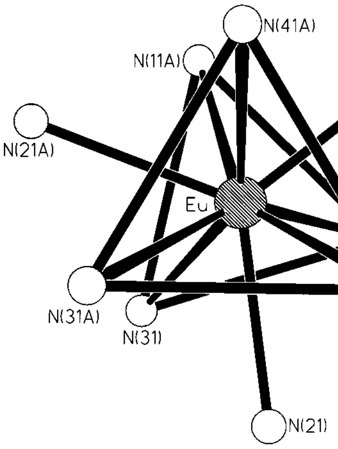

Fig. 8 Co-ordination geometry of the metal centre in $[Eu(L^2)_3][PF_6]_3$

terpyridine), allowing co-ordination of acetonitrile molecules to the metal. Acetonitrile is a relatively poor ligand for lanthanide(III) ions, although adducts are known;[22] it would therefore be expected on the basis of the known oxophilicity of lanthanide(III) ions that potentially co-ordinating O-donor solvents might also induce partial dissociation of polydentate N-donor ligands. The q value obtained for $[Tb(L^1)_2(NO_3)]$ in water suggests four co-ordinated water molecules plus an additional small contribution to quenching from outer-sphere effects; this could be attained by (for example) dissociation of a bidentate arm of one L^1 ligand, or dissociation of some of the terminal pyridyl rings by the conformational rearrangement discussed above, in addition to dissociation of the nitrate ion.

The other types of complex cation based on L^1 that were crystallographically characterised, $[Tb(L^1)_2(H_2O)]^+$ and $[Eu(L^1)_2(dmf)]^+$, will show similar solution behaviour given the labile nature of the monodentate solvent ligands. A more detailed study of the photophysical properties of these complexes is in progress and will be reported separately.

Table 7 Selected bond lengths (Å) and angles (°) for $[M(L^2)_3][PF_6]_3$ (M = Eu, Gd or Ho)

	M = Eu	M = Gd	M = Ho
M–N(11)	2.548(3)	2.526(5)	2.497(2)
M–N(21)	2.599(3)	2.593(5)	2.554(2)
M–N(31)	2.534(3)	2.530(5)	2.482(2)
M–N(41)	2.516(3)	2.504(5)	2.464(2)
M–N(51)	2.577(4)	2.571(7)	2.535(3)
N(41)–M–N(41A)	126.51(14)	127.6(2)	128.01(10)
N(41)–M–N(31A)	149.53(10)	148.8(2)	147.88(7)
N(41)–M–N(31)	77.51(10)	77.4(2)	77.58(7)
N(31A)–M–N(31)	88.35(14)	87.9(2)	87.77(11)
N(41)–M–N(11)	86.98(10)	86.8(2)	86.44(7)
N(41A)–M–N(11)	78.54(9)	78.6(2)	78.78(7)
N(31A)–M–N(11)	79.51(10)	79.9(2)	79.73(8)
N(31)–M–N(11)	125.64(10)	126.1(2)	126.88(7)
N(11)–M–N(11A)	147.56(14)	146.6(2)	145.96(10)
N(41)–M–N(51)	63.26(7)	63.80(11)	64.00(5)
N(31)–M–N(51)	135.82(7)	136.07(11)	136.12(5)
N(11)–M–N(51)	73.78(7)	73.32(11)	72.98(5)
N(41)–M–N(21A)	135.20(9)	135.0(2)	135.25(7)
N(31)–M–N(21A)	73.91(9)	73.4(2)	72.92(7)
N(11)–M–N(21A)	137.81(9)	138.2(2)	138.29(7)
N(41)–M–N(21)	75.62(9)	75.3(2)	74.96(7)
N(31)–M–N(21)	62.75(10)	62.9(2)	63.42(7)
N(11)–M–N(21)	62.96(9)	63.3(2)	63.54(7)
N(51)–M–N(21)	120.82(6)	120.95(11)	120.94(5)
N(21A)–M–N(21)	118.36(13)	118.1(2)	118.12(10)

Synthesis and structures of lanthanide complexes with L^2

Reaction of L^2 with a range of lanthanide salts in methanol, followed by treatment of the resultant solutions with aqueous KPF_6, resulted in formation of the homoleptic complexes $[M(L^2)_3][PF_6]_3$ in good yields. These were characterised on the basis of their elemental analyses and FAB mass spectra (Table 1). The FAB spectra were interesting in that as well as the expected ML^2_n fragments, co-ordinated fluoride ions (arising from the hexafluorophosphate) could be seen, with one or more of the acidic pyrazole groups losing protons as required to give a +1 charge. Thus, peaks corresponding to $[M(L^2)_2F_2]^+$, $[ML^2(L^2 - H)F]^+$ and $[M(L^2 - H)_2]^+$ occurred in every case. We have previously structurally characterised a europium(III) complex in which a co-ordinated fluoride was extracted from a hexafluorophosphate ion.[7]

Three of these complexes (M = Eu, Gd or Ho) were structurally characterised, and are essentially isostructural and isomorphous. Bond lengths and angles for all three are summarised in Table 7. The structure of one example (M = Eu) is shown in Fig. 7. The metal ion is nine-co-ordinate from three terdentate ligands, with a tricapped trigonal-prismatic geometry (Fig. 8). The two triangular faces of the trigonal prism are formed by the two sets of three pyrazolyl N-donor atoms, with the pyridyl donor atoms being the three caps. These planes are not exactly eclipsed but are slightly staggered; however they are almost exactly parallel, with angles between them of 0.6° in each case. All three complexes crystallise in the space group *C*2/*c*, with a C_2 axis along the N(51)–M bond. The terdentate ligands are not exactly planar, but have slight twists between the adjacent aromatic rings. For M = Eu the dihedral angles between the mean planes of adjacent aromatic rings are as follows: between rings 1 and 2, 13.5°; between rings 2 and 3, 11.6° in the same sense; between rings 4 and 5, 8.7° [where ring 1 means atoms N(11) to C(15), and so on]. The absence of any stereoelectronic requirement for octahedral or planar geometry means that the ligands co-ordinate in a strain-free manner with bite angles of *ca.* 61–63° between adjacent rings, in contrast to the values of 70–80° that would be expected with most d-block metal ions. These structures are very similar to those of the homoleptic nine-co-ordinate lanthanide complexes that have been characterised with architecturally similar ligands such as terpyridine and its relatives.[8–11]

Solution luminescence properties of $[Tb(L^2)_3][PF_6]_3$

The luminescence lifetimes τ for $[Tb(L^2)_3][PF_6]_3$ in various solvents are summarised in Table 6. In CH_2Cl_2 (in which the compound is only sparingly soluble) the electronic spectrum showed the expected ligand-centred $\pi \longrightarrow \pi^*$ transitions at $\lambda_{max} = 300$ (maximum) and 260 nm (shoulder). Irradiation at either of these wavelengths produced the typical sequence of $^5D_4 \longrightarrow {}^7F_n$ transitions in the emission spectrum, with the $n = 6$, 5, 4 and 3 components being visible, and a lifetime τ of 1.46 ms.

The difference between the lifetimes in MeOH and CD_3OD ($\tau = 1.09$ and 1.18 ms respectively) gives $q = 0.6$ from the Horrocks equation. This is consistent with the nine-co-ordinate structure being retained in solution, and second-sphere co-ordination of methanol providing the limited amount of solvent-based quenching that occurs. We note that the non-co-ordinated pyrazolyl NH fragments at position 1 of the pyrazolyl rings provide sites for hydrogen bonding with solvents, which could contribute significantly to second-sphere solvation effects.

In water and D_2O however the behaviour is very different. The emission decays are not exactly single exponential [plots of ln(intensity) *vs.* time are slightly curved], indicating a mixture of at least two species with different lifetimes. Consequently the values of τ derived from these data are rather approximate, but the substantial difference between them (0.45 and 0.88 ms in water and D_2O respectively) gives $q \approx 4.6$. As with $[Tb(L^1)_2(NO_3)]$ (above) and $[Eu(terpy)_3]^{3+}$,[21] dissolution of $[Tb(L^2)_3][PF_6]_3$ in water results in partial dissociation of some of the chelating ligands to allow co-ordination of about four or five water molecules. The non-single-exponential decay observed suggests that two or more species, with different extents of hydration and different emission lifetimes, are present and that interconversion between them is slow on the timescale of the luminescence experiment. The dramatic differences between the behaviour of $[Tb(L^2)_3][PF_6]_3$ in water and methanol mirrors that of $[Tb(L^1)_2(NO_3)]$ (above). Clearly water is a much better donor to the metal centre in these complexes than is methanol, with water able to effect partial displacement of the N-donor chelating ligands from the co-ordination sphere of the metal, but methanol not able to do so.

Acknowledgements

We thank the EPSRC for financial support.

References

1 E. Soini, I. Hemmilä and P. Dhalen, *Ann. Biol. Chem.*, 1990, **48**, 567; J.-C. G. Bünzli, in *Lanthanide Probes in Life, Chemical and Earth Sciences, Theory and Practice*, eds. J.-C. G. Bünzli and G. R. Choppin, Elsevier, Amsterdam, 1989, p. 219; A. K. Saha, K. Kross, E. D. Kloszewski, D. A. Upson, J. L. Toner, R. A. Snow, C. D. V. Black and V. C. Desai, *J. Am. Chem. Soc.*, 1993, **115**, 11 032; V. M. Mukkala, M. Heleniu, I. Hemmilä, J. Kankare and H. Takalo, *Helv. Chim. Acta*, 1993, **76**, 1361; M. J. P. Leiner, *Anal. Chim. Acta*, 1991, **255**, 209; A. P. de Silva, H. Q. N. Gunaratne and T. E. Rice, *Angew. Chem., Int. Ed. Engl.*, 1996, **35**, 2116; M. A. Mortellaro and D. G. Nocera, *J. Am. Chem. Soc.*, 1996, **118**, 7414.

2 S. H. Koenig and R. D. Brown, *Prog. Nucl. Magn. Reson. Spectrosc.*, 1990, **22**, 487; R. B. Lauffer, *Chem. Rev.*, 1987, **87**, 901; D. Parker, *Chem. Br.*, 1994, 818; A. D. Watson, *J. Alloys Compd.*, 1994, **207/208**, 14; S. Aime, M. Botta, S. G. Crich, G. B. Giovenzana, G. Jommi, R. Pagliarin and M. Sisti, *J. Chem. Soc., Chem. Commun.*, 1995, 1885; M. Inoue, R. E. Navarro, M. Inoue and Q. Fernando, *Inorg. Chem.*, 1995, **34**, 6074; D. E. Reichert, R. D. Hancock and M. J. Welch, *Inorg. Chem.*, 1996, **35**, 7013; E. Tóth, S. Vauthey, D. Pubanz and A. E. Merbach, *Inorg. Chem.*, 1996, **35**, 3375; D. H. Powell, O. M. Ni Dhubhghaill, D. Pubanz, L. Helm, Y. S. Lebedev, W. Schlaepfer and A. E. Merbach, *J. Am. Chem. Soc.*, 1996, **118**, 9333; G. R. Choppin and K. M. Schaab, *Inorg. Chim. Acta*, 1996, **252**, 299.

3 C. Piguet, J.-C. G. Bünzli, G. Bernardinelli, G. Hopfgartner and A. F. Williams, *J. Am. Chem. Soc.*, 1993, **115**, 8197; C. Piguet, J.-C. G. Bünzli, G. Bernardinelli and A. F. Williams, *Inorg. Chem.*, 1993, **32**, 1237; C. Piguet, J.-C. G. Bünzli, G. Bernardinelli, C. G. Bochet and P. Froidevaux, *J. Chem. Soc., Dalton Trans.*, 1995, 83; C. Piguet, G. Hopfgartner, A. F. Williams and J.-C. G. Bünzli, *J. Chem. Soc., Chem. Commun.*, 1995, 491; C. Piguet, E. Rivara-Minten, G. Bernardinelli, J.-C. G. Bünzli and G. Hopfgartner, *J. Chem. Soc., Dalton Trans.*, 1997, 421.

4 J.-M. Lehn, *Supramolecular Chemistry*, VCH, Weinheim, 1995, pp. 92–95 and refs. therein; P. R. Selvin, J. Jancarik, M. Li and L.-W. Hung, *Inorg. Chem.*, 1996, **35**, 700; A. Døssing, H. Toftlund, A. Hazell, J. Bourassa and P. C. Ford, *J. Chem. Soc., Dalton Trans.*, 1997, 335.

5 D. Parker and J. A. G. Williams, *J. Chem. Soc., Dalton Trans.*, 1996, 3613.

6 W. D. Horrocks and D. R. Sudnick, *Acc. Chem. Res.*, 1981, **14**, 384; N. Sabbatini, M. Guardigli and J.-M. Lehn, *Coord. Chem. Rev.*, 1993, **123**, 201.

7 P. L. Jones, A. J. Amoroso, J. C. Jeffery, J. A. McCleverty, E. Psillakis, L. H. Rees and M. D. Ward, *Inorg. Chem.*, 1997, **36**, 10.

8 G. H. Frost, F. A. Hart and N. B. Hursthouse, *Chem. Commun.*, 1969, 1421; D. A. Durham, G. H. Frost and F. A. Hart, *J. Inorg. Nucl. Chem.*, 1969, **31**, 833.

9 C. Piguet, J.-C. G. Bünzli, G. Bernardinelli and A. F. Williams, *Inorg. Chem.*, 1993, **32**, 4139.

10 C. Mallet, R. P. Thummel and C. Hery, *Inorg. Chim. Acta*, 1993, **210**, 223.

11 C. Yang, X.-M. Chen, W.-H. Zhang, J. Chen, Y.-S. Yang and M.-L. Gong, *J. Chem. Soc., Dalton Trans.*, 1996, 1767.

12 Y. Lin and S. A. Lang, *J. Heterocycl. Chem.*, 1977, **14**, 345.

13 T. Buchen, P. Gütlich, K. H. Sugiyarto and H. A. Goodwin, *Chem. Eur. J.*, 1996, **2**, 1134.

14 SHELXTL 5.03 program system, Siemens Analytical X-Ray Instruments, Madison, WI, 1995; Software package for use with the SMART diffractometer; Siemens Analytical X-Ray Instruments, Madison, WI, 1995.

15 S. Trofimenko, J. C. Calabrese and J. S. Thompson, *Inorg. Chem.*, 1992, **31**, 974 and refs. therein.

16 E. Psillakis, J. C. Jeffery, J. A. McCleverty and M. D. Ward, *Chem. Commun.*, 1997, 479.

17 E. Psillakis, J. C. Jeffery, J. A. McCleverty and M. D. Ward, *J. Chem. Soc., Dalton Trans.*, in the press.

18 A. Novak, *Struct. Bonding* (*Berlin*), 1974, **18**, 177.

19 D. A. Bardwell, J. C. Jeffery, P. L. Jones, J. A. McCleverty and M. D. Ward, *J. Chem. Soc., Dalton Trans.*, 1995, 2921.

20 S. Aime, M. Botta, D. Parker and J. A. G. Williams, *J. Chem. Soc., Dalton Trans.*, 1996, 17.

21 R. D. Chapman, R. T. Loda, R. W. Riehl and R. W. Schwartz, *Inorg. Chem.*, 1984, **23**, 1652.

22 J.-C. G. Bünzli, J.-R. Yersin and C. Mabillaud, *Inorg. Chem.*, 1982, **21**, 1471; J.-C. G. Bünzli and A. Nilicic-Tang, *Inorg. Chim. Acta*, 1996, **252**, 221.

Received 24*th February* 1997; *Paper* 7/01297G